J Mater Sci: Mater Electron (2013) 24:861–865
DOI 10.1007/s10854-012-0835-1

Direct current electric field adjustable phase transformation behavior in (Pb,La)(Zr,Ti)O_3 antiferroelectric thick films

Xiujian Chou · Wenping Geng · Yongbo Lv · Jun Liu · Wendong Zhang

Received: 15 June 2012 / Accepted: 7 July 2012 / Published online: 18 July 2012
© Springer Science+Business Media, LLC 2012

Abstract (Pb,La)(Zr,Ti)O_3 antiferroelectric 1.4 μm-thick films have been prepared on Pt (111)/Ti/SiO_2/Si(100) substrates by sol–gel process. The structures and dielectric properties of the antiferroelectric thick films were investigated. The films displayed pure perovskite structure with (100)-preferred orientation. The surface of the films was smooth, compact and uniform. The antiferroelectric (AFE) characterization have been demonstrated by P (polarization)-E (electric field) and C(capacitance)-V (DC bias) curves. The AFE–ferroelectric (FE) and FE-to-paraelectric (PE) phase transition were also investigated as coupling functions of temperature and direct current electric field. With the applied field increased, the temperature of AFE-to-FE phase transition decreased and the FE-to-PE phase shifted to high temperature. The AFE-to-FE phase transition was adjustable by direct current electric field. (Pb,La)(Zr,Ti) O_3 antiferroelectric films have broad application prospects in microelectromechanical systems because of the phase transition.

1 Introduction

Antiferroelectric (AFE) materials are considered that no spontaneous polarization exists and the orientations of the dipoles are alternatively aligned in opposite directions [1]. Under DC electric field, hydrostatic press or temperature, AFE materials exhibit a phase transformation between AFE and ferroelectric (FE) state accompanying with a larger strain or displacement and phase switching current due to changes of the orientations of dipoles. The AFE-to-FE phase transition has received increasing attention because of its potential usage in energy storage, high-strain transducers/actuators and tunable pyroelectric thermal sensors.

In AFE family, $PbZrO_3$ was the first compound identified as an AFE in 1950 [2]. since then Pb-based AFE ceramics and thin films, such as Pb(Zr,Ti)O_3 [3], (Pb,La)(Zr,Ti)O_3 [4], Pb(Zr,Sn,Ti)O_3 [5], (Pb,La)(Zr,Sn,Ti)O_3 [6] and Pb(Nb,Zr,Sn,Ti)O_3 [7] were studied extensively since their unique properties. In our present work (Pb,La)(Zr,Ti)O_3 thick films was chosen due to lower driving voltage than antiferroelectric bulk ceramics and larger displacement than AFE thin films. [8] B.M. Xu [8] reported the preparation process of PNZST and PLZST thick films with different compositions and the electric property as single temperature or electric-field. X.H. Hao [9] covered the electric properties of PLZST thin films on different bottom electrode under temperature and electric-field. Compared with PLZST and PNZST AFE films, PLZT AFE films hold the characteristics, such as more simple compositions, more easily preparation and lower price. And Compared with PZT films, PLZT films had lower phase temperature and lower operation voltage. In our present work (Pb,La)(Zr,Ti)O_3 thick films shows successive AFE-FE-PE phase transition. With increased direct electric field, this phase transition became more and more obvious. The DC electric field was enough large that the PLZT films were in FE state at room temperature. And also the orientation, microstructure and electrical properties of the PLZT films were studied in detail.

X. Chou (✉) · W. Geng · Y. Lv · J. Liu · W. Zhang
Key Laboratory of Instrumentation Science and Dynamic Measurement, North University of China Ministry of Education, Taiyuan 030051, Shanxi, China
e-mail: chouxiujian@nuc.edu.cn

W. Geng · Y. Lv · J. Liu · W. Zhang
Science and Technology on Electronic Test and Measurement Laboratory, Xueyuan Road 3, Taiyuan 030051, Shanxi, China

In this work (Pb,La)(Zr,Ti)O_3 antiferroelectric 1.4 μm-thick films with (100)-preferred orientation were prepared on Pt (111)/Ti/SiO_2/Si (100) substrates by sol–gel process. The AFE characterization was tested by P (polarization)-E (electric field) and C (capacitance)-V (DC bias) curves. The AFE-to-FE and FE-to-PE transitions were measured as coupling functions of temperature and direct current electric field. In the end, we have given the phase diagram of (Pb,La)(Zr,Ti)O_3 AFE thick films according to the results of the measurements and discussed the dielectric properties as coupling functions in detail.

2 Experimental details

The $(Pb_{0.97}La_{0.02})(Zr_{0.95}Ti_{0.05})O_3$ (PLZT) thick films studied in the present work were prepared by sol–gel process. The precursor materials were lead acetate trihydrate [$Pb(CH_3COO)_2{\cdot}3H_2O$], lanthanum acetate hydrate [$La(CH_3COO)_3{\cdot}H_2O$], zirconium propoxide [$Zr(OC_3H_7)_4$] and titanium isopropoxide [$Ti[OCH(CH_3)_2]_4$]. Their molar ratios were determined according to the composition of PLZT. Lead acetate trihydrate was excess with 15 mol % in order to keep content of Pb stable in the thick films since Pb loss occurred during the annealing process. Lead acetate trihydrate, lanthanum acetate hydrate, and acetic acid were mixed and distilled at 110 °C for an hour to remove water. The required amount of zirconium propoxide and titanium is opropoxide were added and mixed for half an hour when the solution was cooled down to room temperature. At the same time, deionized water was added in order to stabilize the solution. Lactic acid was added into the solution as the function of catalyzer and chelation and ethylene glycol was mixed into the solution as a kind of polymerizing agent. All the materials mentioned above must be mixed thoroughly in order to prepare a sol with uniform composition and then the concentration of the PLZT sol was adjusted to about 0.4 M.

Spin coating was adopted in coating the sol onto Pt(111)/Ti/SiO_2/Si(100) substrates. Each layer was coated at 3000 rpm for 20 s and pyrolyzed at 300 and 600 °C for 10 min, respectively. The spin coating and heat treatment were repeated several times to obtain desired thickness. At last a capping layer of 0.4 M PbO precursor solution prepared by lead acetate trihydrate was added and the films were annealed at 700 °C for half an hour to form the perovskite phase. Gold top pads of 0.5 mm in diameter were coated on the film surface by DC sputtering.

Crystal orientation of PLZT thick films was examined by X-ray diffraction (XRD). Microstructure and cross-section of the films were studied using scanning electron microscope (SEM) and atom force microscope (AFM), respectively. The field-induced hysteresis loops of the PLZT thick films were measured by a modified Sawyer–Tower circuit. The temperature and electric field dependence of dielectric properties were tested using an Agilent 4284A LCR meter.

3 Results and discussion

The XRD pattern of the phase characterization and crystal orientation of the PLZT thick films, which were recorded with a step of 0.02 min^{-1} within the 2θ range from 20 to 60°, are shown in Fig. 1. From the pattern, the film exhibits strong peaks at $2\theta = 22$ and $2\theta = 44°$ corresponding to the (100) and (200) peaks, respectively. (110) and (111) peaks can also be observed at $2\theta = 31$ and $2\theta = 37°$. It indicates the PLZT thick films crystallized into the pure perovskite structure with (100)-preferred orientation. In order to obtain a numerical estimation of the (100) orientation of the PLZT thin films, the orientation factor was calculated according to the following equation

$$F = I\,(100)/[I\,(100) + I\,(110) + I\,(111)] \quad (1)$$

According to the Eq. (1), the (100)-orientation factor (F) was 0.92. The films have a high (100)-preferred orientation. This was because PbO of (100)-orientation is crystallized on the substrates due to 15–20 % excess lead, and then induces the films to grow toward the same direction [10].

Figure 2 illustrates the surface AFM morphology of PLZT thick films. The film surface is uniform and smooth without cracks on an area of 20 μm × 20 μm. The grains are uniformly distributed both fine and large together with an average grain size of 385.52 nm. The obtained roughness parameter (Ra) is 1.76 nm. The cross-sectional SEM of the PLZT film is shown in Fig. 3. The thickness of the film is estimated approximately 1.4 μm.

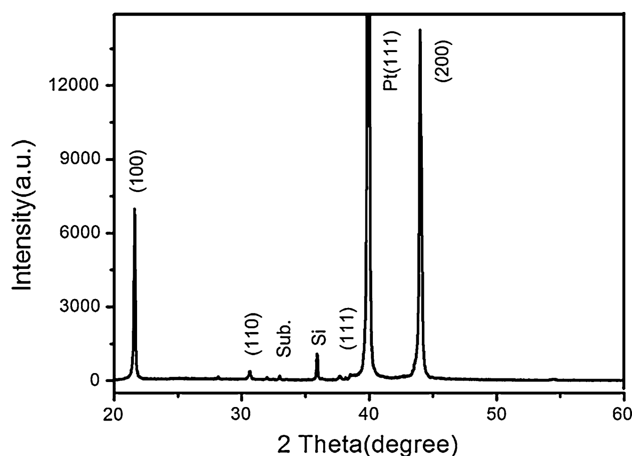

Fig. 1 XRD pattern of PLZT antiferroelectric thick films

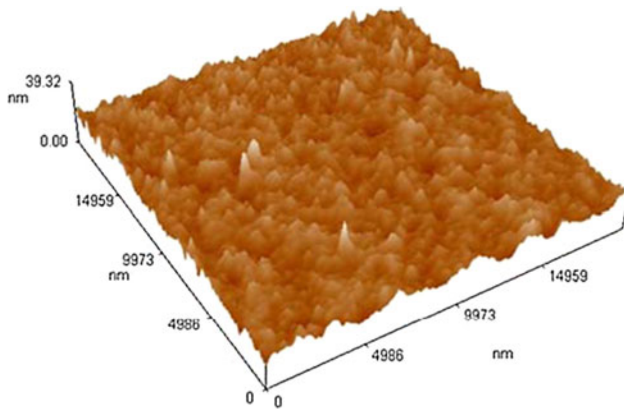

Fig. 2 AFM images of PLZT antiferroelectric thick films

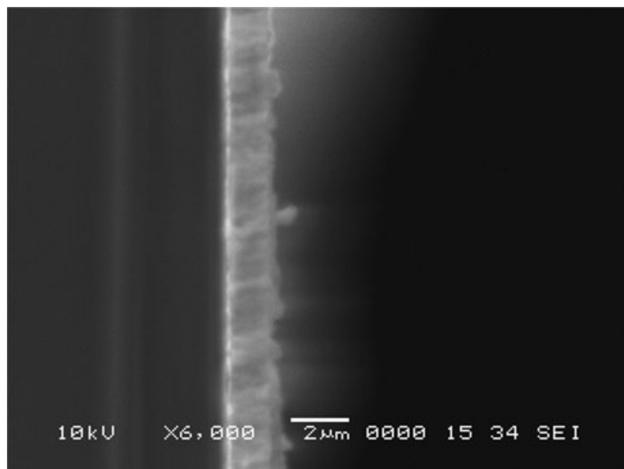

Fig. 3 Cross-section (SEM) images of PLZT anti-ferroelectric thick films

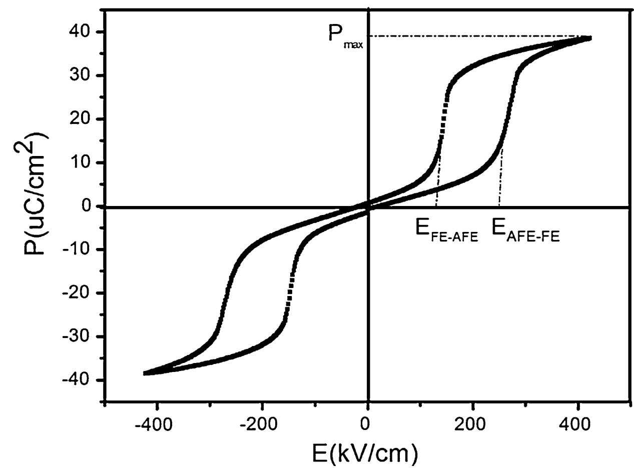

Fig. 4 The hysteresis loops of PLZT antiferroelectric thick films

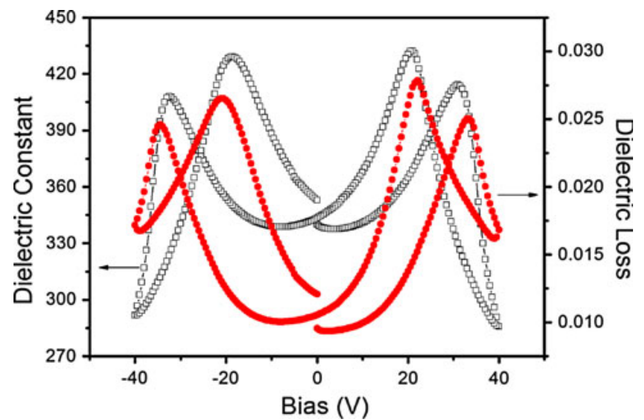

Fig. 5 Dielectric constant and dielectric loss of PLZT antiferroelectric thick films as a function of DC bias

The electric-field-induced phase transformation from AFE to FE phase of the PLZT thick film was investigated. As shown in Fig. 4, The P-E curves were measured at 100 Hz at room temperature. The double hysteresis loops demonstrates the AFE nature of PLZT thick films. They were translated into the FE phase in electric field. Under applied field, the arrangement of dipole changed from antiparallel AFE state into parallel FE state and simultaneity the structure changed dramatically. As the electric field increasing, the polarization showed a sharp phase switching between AFE and FE Phases. The films show a square hysteresis loop. Under maximum field, the value of maximum polarization (Pmax) of the film was about 39 μC/cm^2. The phase transition fields between AFE and FE phase were measured by extrapolating the steepest sections of the hysteresis loop and obtaining their intersections with horizontal axis. The values of forward (AFE-to-FE) phase switching field (E(AFE-FE))and backward (FE-to-AFE) phase switching field (E(FE-AFE)) were 227 and 116 kV/cm, respectively. The double hysteresis loops resulting from the field-forced AFE to FE phase transformation are useful for microdevices.

The dielectric constant and dielectric loss of the PLZT thick films as a function of DC bias are depicted in Fig. 5. It should be noted here that the measurements were conducted at 100 kHz at room temperature, and the maximum DC voltage was 40 V. The voltage was slowly stepped through 0.5 V increments in a cyclic manner from 0 to E_{max}, then E_{max} to $-E_{max}$, and finally $-E_{max}$ to 0. The film shows the double-butterfly C–V curves. The C–V curves show the forward and reverse switching fields of the phase transformation which were the fields from AFE to FE phase transformation and from FE to AFE phase transformation, respectively. The voltages of the AFE to FE transition and the reverse FE to AFE transition were about 31 and 21 V, corresponding to the fields were approximately 221 and 150 kV/cm, respectively. These results from the C–V measurements were not in very close agreement with the P-E analysis on the same films. The various phase

transition field values might result from the two different measurement mechanisms [11]. C–V curves were measured with a DC bias and a weak AC wave, but the P-E curves were measured with a triangle wave. However, like P-E tests, C–V measurements changed the direction of dipoles by an applied field on the general principle.

The dielectric properties were studied under temperature and electric coupling field. With temperature increased, the thermal motion of each cell aggravated and the direction of electric dipole moment in AFE domain was damaged to a certain extent. Under applied electric field, dipoles with a certain degree of freedom overcome the state of disorder due to the thermal motion and turn the orientation to the direction of the electric field. The films were in FE state at the moment [9] When the temperature reached Curie temperature, the domains were destroyed completely and ferroelectricity disappeared. As temperature increased, there were not dipoles from domains which were influenced by applied field. There existed only thermal motion in films and the dielectric constant of the films must obey Curie–Weiss Law. Fig. 6 shows the dielectric constant of PLZT thick films as a function of temperature for various DC electric fields at 100 kHz. It can be obviously seen in Fig. 6a that with the field increasing, the dielectric constant decreased. The Curie temperatures of the films under DC bias of 0, 5 and 10 V were about 140, 125 and 120 °C, respectively. Under 0 V bias, the first transition from AFE to FE phase and the transition from FE to PE phase were occurred nearly the same temperature at about 140 °C and the two transitions were adding together. As the electric field increased, the AFE-to-FE and FE-to-PE transition did not occur at the same temperature and the region of FE phase enlarged very slowly. However, the region of FE phase was so narrow that we can only observe one peak when the two curves of the AFE-to-FE and FE-to-PE transition added together. At the same time, the AFE-to-FE transition is the primary action rather than the FE-to-PE transition. As a result of that, the temperature of the peak in the films decreased.

As shown in Fig. 6b, the AFE-to-FE and FE-to-PE transition was observed at different temperatures with the DC bias between 15 and 30 V. With the field increasing, the temperature of the AFE-to-FE transition shifted to low temperature while the Curie temperature was increasing. The region of FE phase enlarged gradually and so the interaction between AFE-to-FE and FE-to-PE transition lowered at a certain extent [12].

In Fig. 6c, as the field increased above 30 V, the AFE-to-FE transition shifted to lower temperature below room temperature, in other words, the films have been induced to FE phase at room temperature. The only peak was the FE-to-PE transition. Table 1 shows the temperatures of AFE-FE and FE-PE phase transition adjusted by applied DC voltage. All the date comes from Fig. 6. Figure 7 shows phase diagram of the PLZT films as coupling function of DC bias and temperature according to Table 1. The phase change of the PLZT films between the AFE state and the FE state or between the FE state and the PE state can be

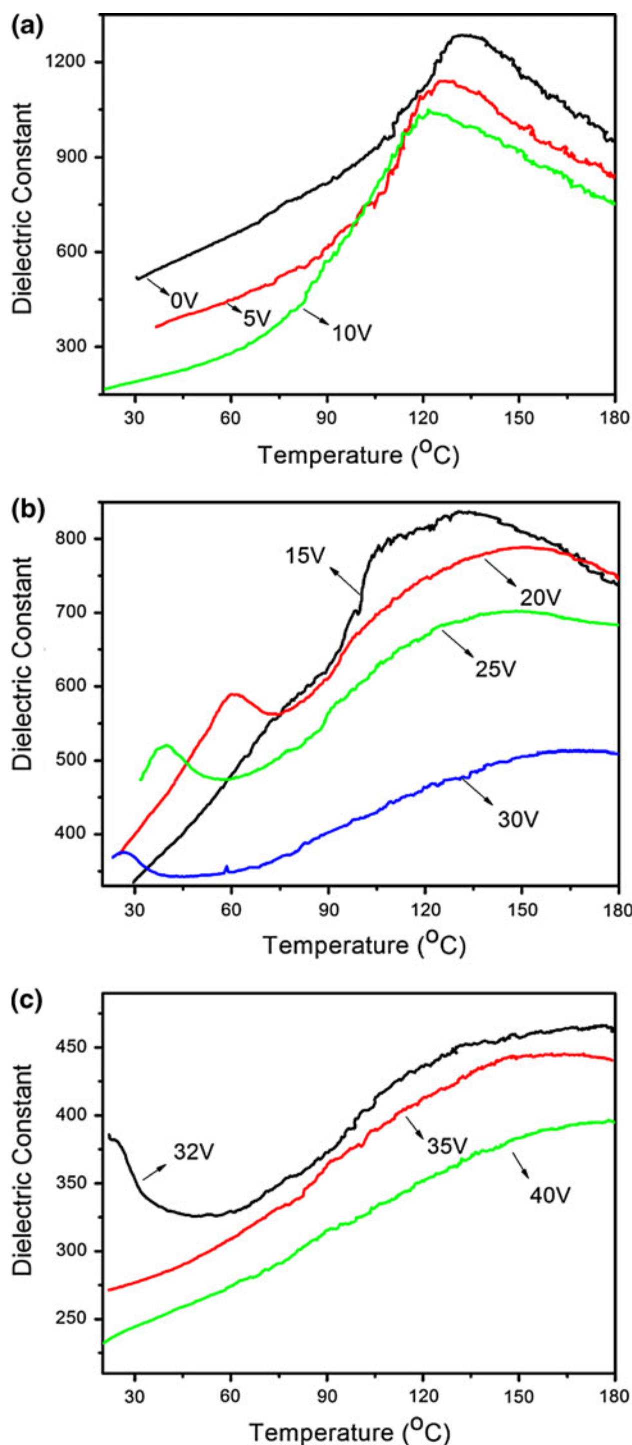

Fig. 6 Temperature dependence of the dielectric constant of PLZT antiferroelectric thick films at different DC bias **a** (0, 5 and 10 V) **b** (15, 20, 25 and 30 V) and **c** (32, 35 and 40 V)

Table 1 The temperatures of AFE-FE and FE-PE phase transition adjusted by applied DC voltage

DC voltage (V)	DC electric field (kV/cm)	Temperature of the AFE-FE phase transition (°C)	Temperature of the AFE-FE phase transition(°C)
0	0	132	132
5	35.7	126	126
10	71.4	122	122
15	107.1	105	133
20	142.9	60	151
25	178.6	40	156
30	214.3	27	167
35	250	–	170
40	285.7	–	178

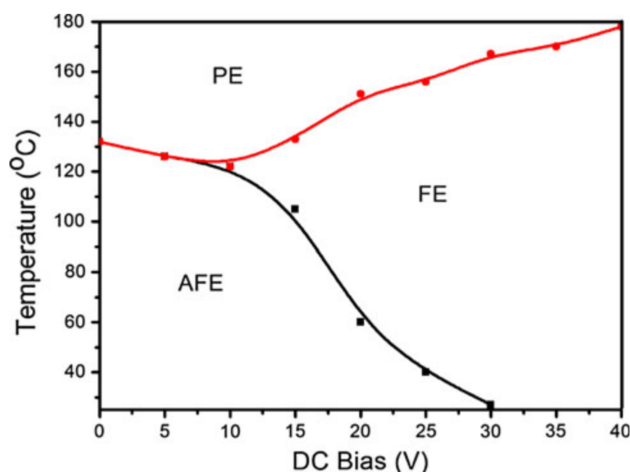

Fig. 7 Phase diagram of the PLZT films as coupling function of DC bias and temperature

adjusted by the coupling function of DC bias and temperature.

4 Conclusions

The successive AFE-FE-PE phase transition was adjusted by direct current electric field. At first, the AFE-to-FE and FE-to-PE transition were adding together. With the applied field increasing, the AFE-to-FE and FE-to-PE transition was observed and the FE phase region was enlarged gradually. When the voltage was 32 V, corresponding to the field reached 229 kV/cm, the films were in FE state at room temperature. This phase transition controlled by applied electric field will play a very important role in microactuator and microsensor.

Acknowledgments The authors would like to acknowledge the support from the National Natural Science Foundation of China under Grant No. 51175483, Shanxi Provincial Natural Science Foundation of China under Grant No. 20100210023-6, and Program for the Outstanding Innovative Teams of Higher Learning Institutions of Shanxi.

References

1. X. Hao, J. Zhai, Composition-dependent electrical properties of (Pb, La)(Zr, Sn, Ti)O3 antiferroelectric thin films grown on platinum-buffered silicon substrates. J. Phys. D Appl. Phys. **40**, 7447–7453 (2007)
2. G. Shirane, E. Sawaguchi, Y. Takagi, Dielectric properties of lead zirconate. Phys. Rev. **84**, 476–481 (1951)
3. R. Seveno, H.W. Gundel, S. Seifert, Preparation of antiferroelectric $PbZr_xTi_{1-x}O_3$ thin films on $LaSrMnO_3$-coated steel substrates. J. Appl. Phys. **79**, 4204 (2001)
4. L.B. Kong, J. Ma, Preparation and characterization of antiferroelectric plzt2/95/5 thin films via a sol–gel process. Mater. Lett. **56**, 30–37 (2002)
5. P. Yang, D.A. Payne, Thermal stability of field-forced and field-assisted antiferroelectric-ferroelectric phase transformations in Pb(Zr, Sn, Ti)O3. J. Appl. Phys. **71**, 1361 (1992)
6. T. Tani, D.A. Payne Lead oxide coatings on sol-gel-derived lead lanthanum zirconate titanate thin layers for enhanced crystallization into the perovskite structure. J. Am. Ceram. Soc. **77**, 1242 (1994)
7. J. Zhai, M.H. Cheung, Z.K. Xu et al., Dielectric and ferroelectric properties of highly oriented (Pb, Nb)(Zr, Sn, Ti)O 3 thin films grown by a sol–gel process. J. Appl. Phys. **81**, 3621 (2002)
8. X. Baomin, L. Eric Cross, D. Ravichandran, Synthesis of Lead zirconate titanate stannate antiferroelectric thick films by sol–gel processing. J. Am. Ceram. Soc. **82**, 306–312 (1999)
9. X. Hao, J. Zhai, X. Chou et al., The electrical properties and phase transformation of PLZST 2/85/13/2 antiferroelectric thin films on different bottom electrode. Solid State Commun. **142**, 498–503 (2007)
10. San.-Yuan. Chen, I.-Wei. Chen, Temperature-time texture transition of Pb(ZrxTi1-x)O3 thin films: i, role of Pb-rich intermediate phase. J. Am. Ceram. Soc. **77**(9), 2332–2336 (1994)
11. X. Li, J. Zhai, H. Chen, (Pb, La)(Zr, Sn, Ti)O3 Antiferroelectric thin films grown on LaNiO3-buffered and Pt-buffered silicon substrates by sol-gel processing. J. Appl. Phys. **97**, 024102 (2005)
12. J. Zhai, H. Chen, E.V. Colla et al., Direct current field adjustable ferroelectric behaviour in (Pb, Nb)(Zr, Sn, Ti)O3 antiferroelectric thin films. J. Phys. Condens. Matter **15**, 963–969 (2007)